THE AMERICAN MINERALOGIST, VOL. 50, MAY–JUNE, 1965

STRUCTURAL DISCONTINUITIES IN THE PLAGIOCLASE FELDSPAR SERIES

R. C. DOMAN[1], C. G. CINNAMON AND S. W. BAILEY,
Department of Geology, University of Wisconsin, Madison, Wisconsin.

ABSTRACT

Optical and x-ray data measured on the same plagioclase grain have been plotted as functions of each other in order to avoid compositional scatter between grains. In the plot of the reciprocal angle γ^* relative to the α refractive index the experimental points for plagioclases in the low structural state lie on nearly linear segments separated from one another by discontinuities near An_{33}, An_{50}, and An_{90-95}. These same discontinuities show up in the plots of the γ^* angle and of the positions of non-Bragg subsidiary reflections as functions of individual grain compositions.

Along each of the linear segments it is proposed that Ca and Al substitute randomly for Na and Si over one or more, but not all, of the available sets of atomic positions. At compositions providing simple Na:Ca and Si:Al ratios, namely An_{33} and An_{50}, reorganization takes place to provide ordering of Na and Ca and regular alternation of Si and Al over as many sets of tetrahedral positions as allowed by the composition and symmetry. An $_{90-95}$ appears to represent the boundary between transitional anorthite and primitive anorthite. The regions of structural reorganization can be correlated with changes at these compositions in a number of optical and physical properties of low plagioclases. These include refractive indices, birefringence, optic angle, orientation of optic plane and optic axes, orientation of rhombic section, wave length of infrared absorption bands, microhardness, types of non-Bragg subsidiary x-ray reflections, and x-ray powder pattern spacings.

INTRODUCTION

Prior to 1934 the plagioclase feldspar series was considered an ideal example of a continuous solid solution series. Taylor *et al.* (1934) provided the first x-ray evidence of structural discontinuity by demonstrating the presence of single subsidiary layer lines between the principal layer lines of Z axis rotation photographs of anorthite. This observation requires that the c repeat of the anorthite end member be twice as large as that of the albite end member. High, low, and intermediate structural forms, similar to those in the potassic feldspars and equated primarily with differences in crystallization and cooling rates, have been recognized since that time. Several additional complexities involving unmixing, non-Bragg subsidiary reflections, and symmetry changes have also been confirmed within the low series. Our present state of knowledge concerning the structural phases present within the low series is summarized in Fig. 1.

The present study reports new optical and x-ray measurements of low plagioclase. Discontinuities in unit cell geometry found within the series

[1] Present address: Ceramic Research Division, Corning Glass Works, Corning, New York.

are interpreted in terms of the ordering patterns of Si, Al and Na, Ca that are possible at certain favorable compositions.

Experimental

Table 1 lists the 39 specimens employed in this study. Several crystals, 0.1 to 0.5 mm in each direction, were selected from each specimen on the basis of optical clarity, uniform thickness, and good cleavage. Grains containing visible imperfections or impurities were excluded. With the exception of specimens U and J at the anorthite end of the series, the samples were selected to represent the low structural state, so far as it is possible to judge from the rock types involved. We hope thereby to reduce to a minimum any variations that may occur as a consequence of a sample's position between the high-low states. A wide variety of rock types is represented in order to avoid undue bias from any one petrologic type. No compositions within the two-phase peristerite region An_{3-14} were investigated.

The refractive indices of the grains were determined by the double variation method on a 5-axis universal stage. Directly measured refractive indices are considered more reliable than indices determined either by rotation from a prime ray or by calculation from the optic angle or the birefringence. For this reason an attempt was made to orient the grains manually so that the same refractive index could be read directly for all grains. The α refractive index was chosen for this purpose. Each grain was mounted on a spindle mount (Wilcox, 1959) in order to facilitate recovery for x-ray study of the same grain. X-ray oscillation and precession photographs were taken of most grains. The positions of the non-Bragg subsidiary type "e" reflections were measured on the oscillation photographs and the reciprocal angle γ^* on the precession photographs.

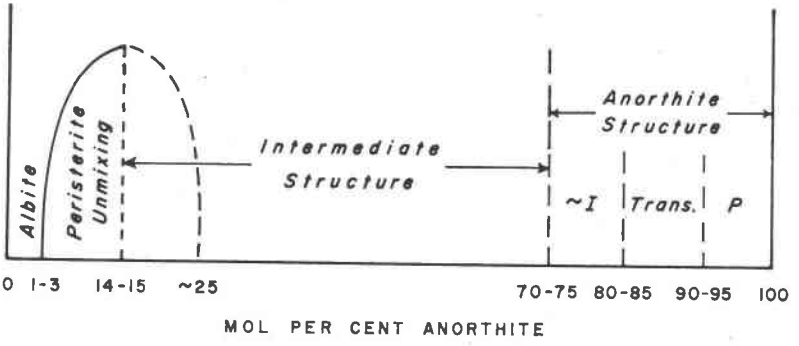

Fig. 1. Schematic representation of the structural types present in the plagioclase series for the low structural state.

TABLE 1. GENERAL DESCRIPTION OF SAMPLES

Sample Number	Previous Number	Source* of Data	Locality	Rock Type	Reported Mol % An
3	Fd-73	1	Parishville, N. Y.	Biotite granite	15.2
5	94	1	Tigerton, Wis.	Granite	18.6
6	152	1	Spanish Peak, Calif.	Gneissoid granodiorite	34.6
8	144	1	Crestmore, Calif.	Granodiorite	36.6
9	24	1	Essex Co., N. Y.	Anorthosite	47.7
10	132	1	Shelby, N. C.	Hornblende gabbro	50.2
11	151	1	Fresno Co., Calif.	Diorite	50.8
12	97	1	Eland, Wis.	Anorthosite	54.5
13	92	1	Tigerton, Wis.	Anorthosite	54.9
15	53	1	E. of Duluth, Minn.	Anorthosite	58.6
16	132	1	Shelby, N. C.	Hornblende gabbro	59.0
17	52	1	Grand Marais, Minn.	Anorthosite	63.2
20	22	1	Wichita Mts., Okla.	Orthoclase quartz gabbro	69.2
21	51	1	Duluth, Minn.	Gabbro	69.2
22	54	1	Grand Marais, Minn.	Anorthosite	69.5
23	165	1	Lincoln Co., Wis.	Gabbro	72.7
25	1A	1	Split Rock Point, Minn.	Anorthosite	76.2
26	Fd-109	1	Rustenberg, Transvaal, S. Africa	Norite	77.0
27	166	1	Merrill, Wis.	Troctolite	80.6
28	D-638	1	Macon Co., N. C.	From vein of talc-anthoph.-plagio. that cuts dunite.	29.8
31	D-761-3	1	Amelia, Va.	Pegmatite	0.4
32	D-761-4	1	Bakersville, N. C.	Pegmatite	19.5
R-1	—	2	Auburn, Maine	—	2.8
EB-18	—	3	Montana	Gabbro	85.8
EB-38	—	3	Montana	Norite	80.0
EB-41	—	3	Montana	Gabbro	62.5
7510	—	H. H. Hess	Bushveld	—	76.0
HGIF-53	—	H. S. Yoder, Jr.	N.W. Greenland	Vein in hornblende actinolite schist	88.7
Ex	—	U. Wis. Coll.	Essex Co., N. Y.	Anorthosite	—
S	43046	U. Wis. Coll.	Labrador	—	—
L	43130	U. Wis. Coll.	—	—	—
U	—	U. Wis. Coll.	Usami, Japan	Basic Lava	—
M	19303	U. Wis. Coll.	Monte Somma, Italy	Amphibolite	—
J	—	R. E. Wilcox	Great Sitkin Island, Aleutians	Basic lava	
V-4	—	T. A. Vogel	Highlands Gneiss, Conn.	Granitic gneiss	—
Fd-44	—	R. C. Emmons	Georgetown, Colo.	Granite	—
Fd-26	—	R. C. Emmons	Gunnison, Colo.	Biotite granite	—
GD-1805	—	G. A. Desborough	Shepherd Mtn., Missouri	Ferrogabbro	—
JC-21	—	U. Wis. Coll.	Tan Trough Mica Mine, Yancey Co., N. C.	Pegmatite	—

* References for Source of Data:

1. R. C. Emmons (1953).
2. P. H. Ribbe (1960).
3. J. R. Smith (1960).

The reciprocal α^* and β^* angles were not measured because they do not change appreciably throughout the plagioclase series. The experimental data are recorded in Table 2.

The estimated probable error of the directly measured refractive indices is $\pm .0005$. In the regions near the structural discontinuities each listed α index is the average of two separate determinations. The measurements of δ_c, the position of the non-Bragg subsidiary type "*e*" reflections on Z axis oscillation photographs, were made with a traveling cross hair and vernier attached to an engraved steel scale. These measurements are estimated to have an accuracy within $\pm 3°$ for compositions An_{33} to An_{80} and $\pm 4°$ to 10° for more sodic compositions. All precession photographs were taken with unfiltered Mo radiation on carefully oriented grains. All angular measurements were repeated from two to six times. The estimated error of measurement of the reciprocal angle γ^* is less than 0°10′.

Results

A plot of experimental data relative to bulk composition, as derived from chemical analysis, involves the possibility of compositional and structural variation from grain to grain within a sample. A resultant scatter of points, such as illustrated by Crump and Ketner (1953), Emmons *et al.* (1960), and Vogel (1964), is encountered frequently with plagioclases. The scatter is real and is present in both the optical and *x*-ray measurements of the present study (Table 2). In order to avoid the effect of compositional variation from grain to grain, the experimental data obtained from the same grain have been plotted with respect to one another rather than with respect to composition. This has the effect of smoothing out compositional scatter, provided the variable parameters are both functions of composition.

Of the measured variables the graph of the variation of γ^* as a function of the α refractive index (Fig. 2) was found to be the most informative in delineating structural breaks in the low plagioclase series. The experimental points lie on linear or nearly linear segments separated by discontinuities at mol per cent values of An_{33-35}, An_{50-52}, and An_{90-95}. There is a slight overlap of the ends of adjacent segments at the first two breaks. The latter break near An_{90} is less well defined and could be interpreted as a flexure rather than a discontinuity. The maximum deviation of any point from the nearest linear segment is approximately equal to the estimated maximum error of measurement of γ^* and α.

The compositional markers were placed in Fig. 2 by cross reference with an average α refractive index curve. For this purpose we have averaged our own measurements with those of Crump and Ketner

TABLE 2. SUMMARY OF *X*-RAY AND OPTICAL DATA

Grain Number	Mol % An Analysis	Refractive Indices					Mol % An Calc.
		α	β	γ	δ_e	γ^*	
R-1c	2.8	1.5284	—	1.5400	—	90.37	0.9
R-1f		1.5297	1.5337	1.5397		90.33	1.9
R-1h		1.5293	1.5339*	1.5398	—	90.20	2.6
3a	15.2	1.5368	1.5406	1.5451	—	89.57	15.0
3b		1.5361	1.5404	1.5451	—	89.55	14.6
3c		1.5359	—	1.5454	—	89.59	13.8
5b	18.6	1.5372	—	—	—	89.37	17.4
5c		1.5384	—	—	—	89.40	18.3
5j		1.5378	—	—	—	89.30	18.8
5l		1.5386	—	—	—	89.22	20.3
5m		1.5387	—	—	—	89.38	18.7
6a	34.6	1.5466	1.5499*	1.5541*	—	88.68	33.9
6b		1.5454	1.5489*	1.5525	—	88.58	33.7
8a	36.6	1.5477	1.5512*	1.5555*	117°	88.83	38.9
8b		1.5463*	1.5497	1.5534	118	88.67	33.7
8c		—	—	—	111	88.88	—
9a	47.7	1.5521	1.5552*	1.5597*	137	—	—
9b		1.5541	1.5570*	1.5607	143	—	—
9c		1.5545	1.5571*	1.5608	142	88.22	52.2
9d		1.5532	1.5563*	1.5604	139	88.37	49.2
10a	50.2	1.5540	1.5570*	1.5615*	137	88.23	51.5
10b		1.5514	1.5543*	1.5587*	133	88.50	46.2
10c		1.5526	1.5557*	1.5600*	134	88.50	47.3
10d		1.5541	1.5570	1.5615*	137	—	—
10e		1.5533	1.5564*	1.5603	136	—	—
11a	50.8	1.5543	1.5574*	1.5620*	140	88.28	51.3
11b		1.5540	1.5570*	1.5614*	137	88.43	49.6
11c		1.5546	1.5577*	1.5625	137	88.38	50.8
11d		1.5538	1.5566	1.5611*	138	88.43	49.2
12a	54.5	1.5550	1.5576	1.5626*	137	—	—
12b		1.5568	1.5600*	1.5646*	137	—	—
12c		1.5566	1.5598*	1.5639	138	—	—
12d		1.5553	1.5582*	1.5628	137	88.43	54.3
12e		1.5563	1.5592*	1.5639*	138	88.40	55.7
12f		1.5562	1.5593*	1.5640*	138	88.35	56.0
12g		1.5545	1.5573*	1.5617	132	88.60	52.0
12h		1.5564	1.5586	1.5640*	133	88.55	54.4
12i		1.5562	1.5586	1.5638*	135	88.38	55.8
12j		1.5568	1.5600*	1.5646*	135	88.60	54.3
13a	54.9	1.5556	1.5584*	1.5630*	134	88.60	53.1
13b		1.5559	1.5588*	1.5633*	133	88.57	53.7
13c		1.5559	1.5588*	1.5637	131	88.57	53.7
13d		1.5566	1.5590	1.5642*	133	88.57	54.4
13e		1.5545	1.5571*	1.5610	130	88.65	51.4
13f		1.5560	1.5586	1.5633*	136	88.37	55.6
15a	58.6	1.5649	1.5701*	1.5751*	180	87.63	74.8
15b		1.5615	1.5646	1.5701*	160	87.97	66.0
15c		1.5632	1.5679*	1.5720	164	—	—
15d		1.5606	1.5643	1.5693*	164	—	—
15e		1.5618	1.5652*	1.5712*	165	87.82	68.1
15f		1.5607	1.5648*	1.5695*	166	—	—
16a	59.0	1.5574	1.5609*	1.5647	141	88.35	57.5
16b		1.5579	1.5610*	1.5649	144	—	—
16c		1.5572	1.5607	1.5646*	143	88.25	58.2

* Rotated indices.

TABLE 2—(*continued*)

Grain Number	Mol % An Analysis	Refractive Indices					Mol % An Calc.
		α	β	γ	δ_c	γ^*	
17a	63.2	1.5615	1.5646	1.5701*	155	88.07	65.3
17b		1.5617	1.5649	1.5702*	159	88.05	65.7
20a	69.2	1.5620	1.5662*	1.5712*	157	87.90	67.5
20b		1.5625	1.5667	1.5721*	157	88.02	66.9
20c		1.5621	1.5657	1.5712*	155	88.05	65.8
21a	69.2	1.5638	1.5683	1.5734*	180	87.77	71.3
22a	69.5	1.5625	1.5670*	1.5719*	180	87.82	69.2
23a	72.7	1.5637	1.5676	1.5730*	159	87.80	71.0
23b		1.5645	1.5681	1.5740*	160	87.65	73.9
23c		1.5646	1.5686	1.5741*	159	87.60	74.8
23d		1.5643*	1.5689	1.5734	163	87.78	72.0
25a	76.2	1.5664	1.5719	1.5771*	180	87.48	78.6
26a	77.0	1.5659	1.5712*	1.5772	160	87.70	75.2
26b		1.5659	1.5711*	1.5762*	164	87.67	75.7
27a	80.6	1.5673	1.5729*	1.5782*	180	87.52	79.4
28a	29.8	1.5442	1.5481*	1.5516	121	88.65	31.9
28b		1.5437	1.5476*	1.5514*	—	88.67	31.2
28c		1.5417	1.5467*	1.5511	—	88.84	27.4
31a	0.4	1.5284	1.5320	1.5386*	—	90.45	0.3
32a	19.5	1.5373	1.5408	1.5455*	—	89.57	15.5
32b		1.5397	1.5435	1.5472*	100	89.20	21.6
32c		1.5377	1.5430*	1.5474	110	89.32	18.5
EB-18	85.8	1.5692	1.5751*	1.5806*	180	87.33	84.9
EB-38	80.0	1.5675	1.5733*	1.5783*	180	87.53	79.6
EB-41a	62.5	1.5595	1.5632*	1.5681*	155	88.17	61.4
EB-41b		1.5605*	1.5647	1.5683	154	—	—
EB-41c		1.5607	1.5644	1.5693*	154	—	—
EB-41d		1.5615	1.5652	1.5703*	156	88.12	64.2
EB-41e		1.5608	1.5644	1.5695*	154	88.17	62.8
7510a	76.0	1.5655	1.5698	1.5754*	159	87.70	74.7
7510b		1.5666	1.5708	1.5768*	161	87.62	77.2
HGIF-53	88.7	1.5704	—	—	—	87.27	87.6
JC-21	—	1.5396	—	—	—	89.22	21.4
Fd-26b	—	1.5420	—	—	—	89.06	25.5
Fd-26c		1.5420	—	—	—	89.07	25.4
Fd-26d		1.5410	—	—	—	89.11	23.9
Fd-26f		1.5375	—	—	—	89.47	16.7
Fd-26h		1.5396	—	—	—	89.26	21.0
Fd-26k		1.5422	—	—	—	89.08	25.3
Fd-26m		1.5395	—	—	—	89.30	20.4
Fd-26n		1.5408	—	—	—	88.99	24.9
Fd-26o		1.5383	—	—	—	89.34	18.8
V-4a	—	1.5440	—	—	—	88.72	30.9
V-4b		1.5444	—	—	—	88.68	31.8
V-4c		1.5440	—	—	—	88.75	30.5
Fd-44	—	1.5447	—	—	—	88.72	31.7
GD-1805a	—	1.5473	—	—	—	88.85	38.2
GD-1805c		1.5475	—	—	—	88.83	38.6
GD-1805d		1.5469	—	—	—	88.86	37.8
GD-1805e		1.5502	—	—	—	88.75	42.5
GD-1805f		1.5470	—	—	—	88.86	37.9
GD-1805g		1.5458	—	—	—	89.05	34.6
GD-1805i		1.5459	—	—	—	89.08	34.3
GD-1805j		1.5464	—	—	—	88.92	36.6
GD-1805k		1.5448	—	—	—	89.07	33.0
Ex-a	—	1.5514	1.5545*	1.5578	129	88.67	44.4

TABLE 2—(*continued*)

Grain Number	Mol % An Analysis	Refractive Indices			δ_c	γ^*	Mol % An Calc.
		α	β	γ			
Ex-b		1.5500	1.5532*	1.5573	121	88.73	42.4
Sa	—	1.5549	1.5573	1.5619*	—	—	—
Sb		1.5537*	1.5563	1.5612	135	—	—
Sc		1.5544	1.5571*	1.5610	134	88.58	52.1
La	—	1.5540	1.5570*	1.5614*	135	88.67	50.7
Lb		1.5545	1.5572*	1.5614	134	88.67	51.2
Lc		1.5541	1.5571*	1.5616	132	88.65	50.9
Ld		1.5544	1.5573*	1.5616	133	88.65	51.3
U	—	1.5736	1.5810*	1.5862*	—	87.15	96.4
M	—	1.5720	1.5793*	1.5840*	—	87.13	91.5
J	—	1.5754	1.5838*	1.5888*	—	87.07	99.7

(1953), Ribbe (1960), and Smith (1960) on the same samples. We assume in this procedure that enough grains have been measured with comparable precision in each sample for the averaged α index to be representative of the bulk composition. After drawing a smooth line of best fit through the plotted average values for the specimens used, the composi-

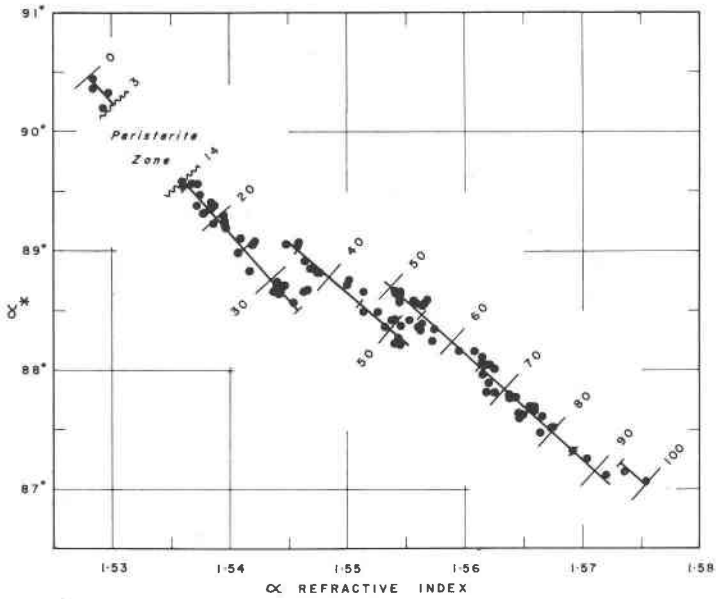

FIG. 2. Variation of reciprocal angle γ^* with respect to the α refractive index measured on the same grain. Compositional markers were placed by cross reference with an average α index curve. Scatter within samples is mainly parallel to the linear segments.

tion corresponding to a given α index could be transferred to the graph of Fig. 2. The published index curves of Crump and Ketner were also used to check the accuracy of the positioning of the composition markers. The two methods agreed within less than one per cent An over most of the curve. A second check utilizing a curve of averaged γ^* values relative to bulk composition also showed close correspondence with the composition markers as given in Fig. 2.

Special mention must be made of the composition in the vicinity of the discontinuities of Fig. 2. In order not to prejudge the presence or absence of corresponding breaks in the refractive index curves, we have intentionally drawn a smooth curve through the points of the average α index curve. In Fig. 2, therefore, a given α index can represent only one composition, even on opposite sides of a discontinuity. It could be argued that the presence of breaks implies that a compositional difference should exist between the ends of adjacent segments. Some evidence for this view can be found in small deviations of points from the average index curve near An_{33} and An_{50}, but the samples are not spaced closely enough together for us to be certain of the exact trend of the curve. For these reasons the compositional markers as now given at the ends of each segment are subject to change.

Figure 2 does not require the use of analyzed specimens for its construction. Accordingly, data from the eleven unanalyzed samples listed at the end of Table 1 have been utilized to fill out those portions of the plot where data from the analyzed samples were scarse. Unfortunately, two of these samples, U and J, are anorthite phenocrysts from lava flows and may reasonably be interpreted as high structural forms. For this reason the small break or flexure at the anorthite end of the curve must be considered tentative until data can be obtained for true low-state anorthites in this region. The similarity in the refractive indices of the high and low forms at the anorthite end (Reynolds, 1952) and the break in the index curves of Smith (1960) around An_{90}, however, provide supporting evidence for the reality of the break as shown. An additional supporting fact is that the γ^* value for the low anorthite whose structure was determined by Kempster, Megaw, and Radoslovich (1962) would fall on our graph at An_{98}. Although an α index is not given, Gay (1953) states that this material is nearly pure anorthite on the basis of refractive index and extinction angle measurements.

The data of J. V. Smith (1956), J. R. Smith (1958), Tomisaka (1959), and Brown (1960*a*) can be combined with measurements of our own on heated and volcanic plagioclases to show that the γ^* angle—α index curve for the high structural state would be a nearly straight, horizontal line having a γ^* angle of $88.0 \pm 0.2°$ from An_0 to An_{67}. At An_{67} the curves

for the low and high structural states join and remain nearly coincident to An_{100}. It is observed in the present study that the scatter of values between grains from the same specimen is predominantly parallel to the linear segments of Fig. 2 rather than normal to them. For compositions An_0 to An_{67}, at least, this scatter must be a result of compositional differences from grain to grain rather than of differences in degree of order. For most specimens the indicated scatter amounts to less than three per cent An because more extreme compositions were eliminated by centrifugation during preparation of the sample for chemical analysis. The maximum compositional variation encountered between grains was 8.8 per cent An for specimens 15 and Fd-26. Specimen 15 is also the only sample in which the compositions of the individual grains do not agree closely with the composition by chemical analysis, the difference amounting to approximately 10 per cent An. Glauser (1961) has also commented that compositions derived optically from thin sections of this specimen do not correspond with the chemical analysis.

In Fig. 3 the γ^* angle is plotted as a function of the β and γ refractive indices. Over half of these indices are rotated values rather than direct measurements. Despite the resultant greater scatter and the smaller number of experimental points, the two curves are very similar to that in

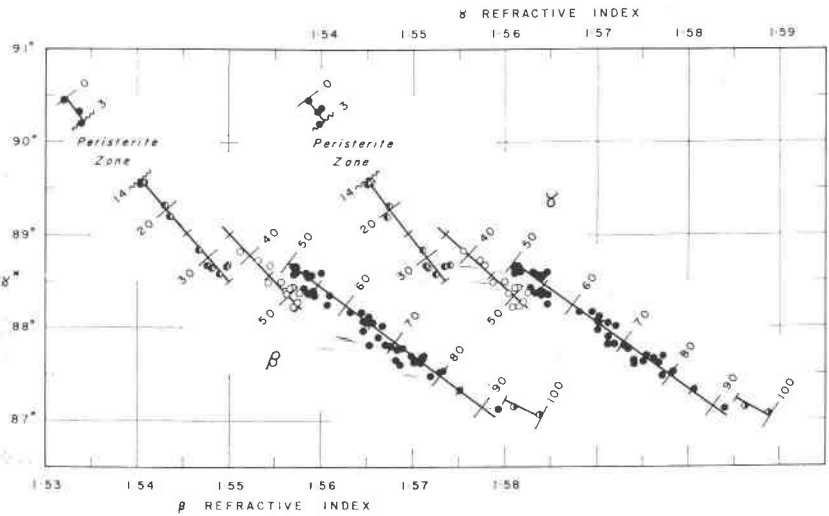

FIG. 3. Variation of reciprocal angle γ^* with respect to the β and γ refractive indices measured on the same grain. Lines through the points and compositional markers were placed by cross reference with Fig. 2. Different symbols are used to distinguish points lying on the different linear segments of Fig. 2.

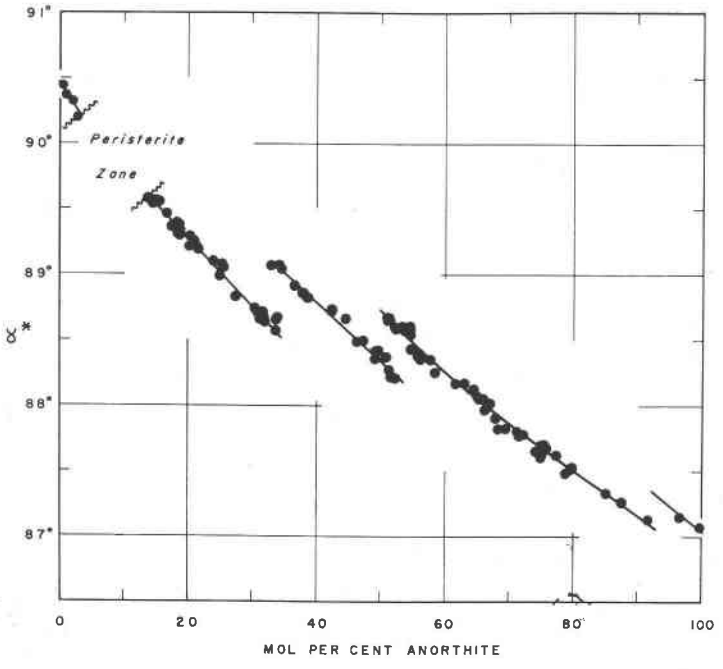

FIG. 4. Plot of reciprocal angle γ^* with respect to individual grain composition. The discontinuities in unit cell geometry are at An_{33-35}, An_{50-52}, and An_{92-96}.

the preceding figure. The lines through the points and the compositional markers were positioned by cross reference with Fig. 2.

Individual grain compositions determined by projecting the individual points normally onto the linear segments of Fig. 2 have been used to construct more precise curves of the variation of γ^* and of the α refractive index as a function of mol per cent anorthite, illustrated in Figs. 4 and 5 respectively. The scatter of γ^* values is reduced substantially in Figure 4 so that the discontinuities in unit cell geometry at An_{33} and An_{50} show up more clearly than in the preceding figures. The lines through the individual points represent the linear segments from Fig. 2 as transferred to this graph point by point. The maximum deviation of any point from its corresponding segment is 0.1°, whereas the difference in γ^* between the ends of adjacent segments is 0.5°. The segment from An_{50} to An_{90} transfers as a slightly concavo-convex curve that could also be interpreted as two straight lines of different slopes joining at about An_{67}. No discontinuities are apparent in the α refractive index curve of Fig. 5, but it must be remembered that this curve is derived from Fig. 2 in which a

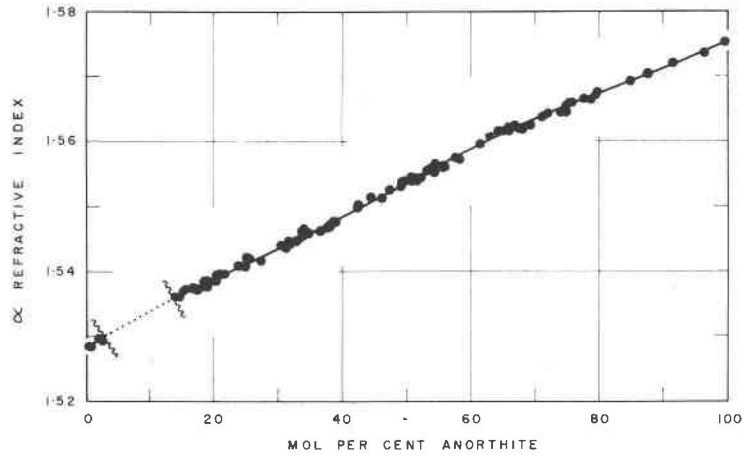

FIG. 5. Plot of α refractive index with respect to individual grain composition. Line through points in an overlay of the average α index curve used to construct the compositional markers in Fig. 2.

smooth variation of index with composition is assumed. The actual α index values in the regions near An_{33}, An_{50}, and An_{90} are subject to change for this reason. The present work suggests that if any discontinuities in index do exist in these regions they will be small. It is also noted that the trend of points in Fig. 5 could be described equally well by a series of straight lines with changes of slope at An_{33}, An_{50}, and An_{67}.

Crump and Ketner (1953) and Ribbe (1960) have suggested a break in the refractive index curves near the sodic end of the two-phase peristerite region. Ribbe (1960) notes that this break at An_{5-7} (wt %) does not correspond exactly with the sodic limit of unmixing at An_{1-3}, whereas in theory it should correspond. A similar situation exists near the calcic end of the peristerite region. Smith (1960) shows a break in his index curves at An_{20} (mol %), whereas no unmixing is observed beyond about An_{14}. We have not attempted to verify either of these optical breaks in the present study. We do note on the basis of Fig. 5 that either a flexure or break would be needed to join An_0 with the trend of the curve beyond An_{14}, but that any deviation from continuity in these regions would have to be quite small, say 0.001 or less. Verification of these suggested breaks will require precise compositional control, perhaps by means of an electron microprobe, for the individual grains used for index determinations.

Brown (1960*b*) and Ribbe (1962) have pointed out another problem that exists at the calcic end of the peristerite zone. No unmixed specimen has ever been recognized in the composition region in which the calcic phase should be predominant, more calcic than $An_{14\pm2}$ where precession photographs show the two phases to be present in approximately equal

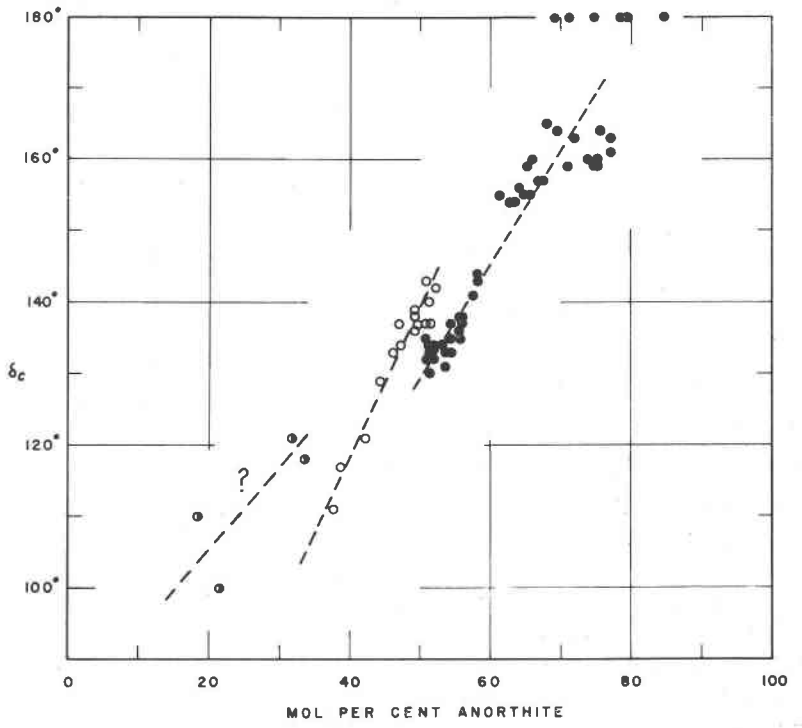

FIG. 6. Plot of position of non-Bragg type "*e*" subsidiary reflections on Z axis oscillation photographs with respect to individual grain composition. Different symbols are used to distinguish points lying on the different linear segments of Figs. 2 and 3.

amounts (Fig. 1). Examples of unmixing on the calcic limb of the solvus appear to be missing. This is verified in our own study in which all specimens more calcic than An_{14} (mol %) were found to be homogeneous.

Figure 6 illustrates the variation in the positions of the non-Bragg subsidiary type "*e*" reflections as a function of individual grain composition. The discontinuities apparent at An_{33} and An_{50} represent differences of nearly 15° between the ends of adjacent segments whereas the estimated error of measurement is less than $\pm 3°$ for An_{33-80}. The position of the most sodic segment is uncertain because of the diffuseness of the subsidiary spots. Values of 180° near the calcic end probably represent Bragg difference reflections of the anorthite type structure rather than non-Bragg reflections. There is more scatter in the positions of the non-Bragg reflections for compositions between An_{60} and An_{80} than would be expected from the estimated error of measurement. The cause for this scatter is not known. A possible interpretation is that there is an additional flexure or discontinuity in the region An_{67-70}.

Interpretation

Intermediate compositions between $NaAlSi_3O_8$ and $CaAl_2Si_2O_8$ have non-integral values of the large cations, Na and Ca, and of the tetrahedral cations, Si and Al, within one formula unit. In an ideal substitutional solid solution these cations must be distributed at random over the corresponding structural positions of different unit cells so that these positions in the "average" unit cell would contain "half-breed" atoms (Na,Ca) and (Si,Al). The physical properties and average unit cell size and shape should vary smoothly with composition. Although there are compositional ranges in the low plagioclase series in which the unit cell shape, expressed by γ^*, does vary smoothly with composition, it is especially significant that these ranges are terminated abruptly at compositions with simple ratios of Na:Ca and Si:Al. At An_{33} the ratio of Na to Ca and of Si to Al is 2 to 1. At An_{50} the Na:Ca ratio is 1:1 and the Si:Al ratio is 5:3.

We interpret the linear segments and discontinuities evident in Figs. 2–4 in the following manner.

1) Along each linear segment random substitution of Al for Si and Ca for Na takes place over one or more sets of equivalent atomic positions. We do not attempt to specify which sets are involved because of the large number of possibilities. For example, in anorthite there are four sets of large cation positions and sixteen sets of tetrahedral positions. In albite and intermediate composition plagioclases the number of sets appears to be reduced to $\frac{1}{4}$ that of anorthite because of higher symmetry and smaller cell volume (albite $C\bar{1}$ with $c \leqq 7$ Å and anorthite $P\bar{1}$ with $c \leqq 14$ Å). In the case of several different plagioclases, however, electron density maps based on an albite-size unit cell have shown distinct signs of atom-splitting. This effect can be interpreted as due to an average structure in which the contents of four slightly different albite-size subcells have been superimposed. Megaw (1962) suggests that the diffraction maxima characteristic of the true, larger cell have been smeared out by an anti-phase domain structure.

2) At compositions that provide simple ratios of Si:Al and Na:Ca, structural reorganization takes place whereby the Si and Al are redistributed in a regular pattern over as many sets of tetrahedral positions as the bulk composition will allow. We assume that Na and Ca order at the same time. Especially at the calcic end of the series, the pattern of Si,Al ordering adopted would be expected to be the regular 1:1 alternation found in anorthite. Thus, for purposes of illustration, at An_{50} the Si:Al ratio of 5:3 is correct for regular alternation of Si and Al over exactly three-fourths of the tetrahedral positions with the remaining positions occupied by Si alone. Although the exact details of the changes that take

place at An_{33} and An_{50} cannot be specified, some major structural reorganization involving cation redistribution appears necessary to explain the large observed change in γ^* of 0.5° between the ends of adjacent linear segments. A small change in refractive index might also be expected from such a reorganization.

3) The experimental data can be interpreted to have either a discontinuity or a flexure in the region An_{90-95}. This is about the boundary between primitive anorthite and transitional anorthite (Fig. 1). It is also about the dividing line between the more calcic specimens that retain a *c* axis periodicity of 14 Å on quenching from temperatures just under the solidus and the more sodic specimens that have a 7 Å *c* axis characteristic of the high structural state (Gay, 1962).

4) There are also discontinuities near An_{33} and An_{50} of the positions of the non-Bragg type "*e*" subsidiary reflections (Fig. 6). Megaw (1960) has explained the non-Bragg reflections as due to stacking faults that nucleate within an ideal intermediate plagioclase structure as a result of atomic misfit inherent in the substitution NaSi—CaAl. Her ideal structure consists of 18 subcells differing from one another in Si,Al pattern and in distortion of the framework structure. The postulated stacking faults would be spaced at intervals of several unit cells and should not directly affect the geometry of the individual subcells. Megaw suggested certain sequences of filling up the tetrahedral positions within the ideal structure, but did not suggest any reorganization of Si,Al distribution except at An_{78}, where the ideal structure was believed to first form. Our data do not show a break at An_{78}.

The observation of discontinuities in the δ_c values eliminates the possibility that some of the effects noted in the present study might be due to use of specimens in intermediate structural states. Gay and Bown (1956) have shown that the positions of the subsidiary reflections do not change on heat treatment. The geologic occurrences of the specimens, the adherence of the points from different specimens to linear segments, and the occurrence of the breaks at simple Na:Ca and Si:Al ratios all suggest that we are dealing with structural changes taking place entirely within the low structural series. Vogel (1964) has especially examined our specimens near An_{33} and An_{50} that would approach closest on a γ^*—α graph to the high structural series. He reports that the poles of recognizable late-stage deformation twins in these specimens fall on the migration curves for the low structural state.

5) The random substitution of Al for Si and of Ca for Na postulated along the linear segments differs from that in the high structural series in that the randomness does not involve as many of the available sets of positions for these elements. However, the high structural series is not

necessarily completely disordered. The similarity of the γ^* curves from An_{100} to An_{67} suggests that the Si,Al distributions may be quite similar over this range for the low and high structural states, but become increasingly different for more sodic compositions. This implies that An_{67} may represent another unique composition with respect to Si,Al distribution. The Na:Ca ratio is 1:2 and the Si:Al ratio is 7:5. Although there is no apparent discontinuity at An_{67} in any of our figures for the low plagioclases, mention has been made in the text of possible small changes of slope at this composition in Figs. 4–6.

The discontinuities observed in the present study can be correlated with changes at these same compositions in a number of optical and physical properties of low plagioclases recorded in the literature. The possible breaks in the refractive index curves near the boundaries of the peristerite region have already been mentioned. Smith (1960) shows a break at $An_{90\pm3}$ in refractive index, birefringence, and optic angle curves and a reversal of slope in the optic angle curve at An_{52}. Van der Kaaden (1951) shows the optic angle reversal closer to An_{50}. Duparc and Reinhard (1924) show prominent changes in slope near An_{35} and An_{52} in curves of the angle between the optic plane and (001) for sections normal to optic axis B and in stereographic projections of the optic axes onto planes normal to the crystallographic axes. The curves of the variation of microhardness with composition (Mookherjee and Sahu, 1960) show a change in slope near An_{52} for loads not exceeding 100 grams. The samples are not spaced closely enough together to define accurately a second change of slope that occurs somewhere between An_{25} and An_{40}. Thompson and Wadsworth (1957) have found a marked flexure (bathochromic shift) between An_{31} and An_{35} in the wave length of the infrared absorption band in the 15.4–16.2 micron region. The non-Bragg type "*e*" reflections become diffuse at compositions more sodic than An_{33} and the type "*f*" reflections are found only for compositions more calcic than An_{50-55} (Bown and Gay, 1958).

The differences between the spacings of adjacent reflections on *x*-ray powder photographs have been used extensively to determine composition and structural state for the plagioclase feldspars (Goodyear and Duffin, 1954; Smith and Yoder, 1956; Smith and Gay, 1958). Changes in the relative spacings of the particular reflections used are primarily dependent on the variation of the γ^* angle with composition and structural state. For this reason the spacing graphs for the low plagioclases show a general similarity to the γ^* graphs in this paper with steep slopes at the two ends of the series and flattening out in the region An_{35} to An_{50}. J. V. Smith (1958) has also pointed out that the position of the rhombic section varies in a similar manner because of its dependence on the value

of the crystallographic angle γ. The present study suggests that the existing x-ray spacing graphs must be modified in the region An_{30} to An_{50} to show the observed discontinuities. The overlapping of γ^* values near An_{33} and An_{50} will make the interpretation of the observed spacings additionally ambiguous in these regions in terms of trying to separate the effect of composition as opposed to structural state. For a given composition the high and low structural states differ primarily in their γ^* values. Our data now indicate that plagioclases of very similar compositions can have differences in γ^* of 0.4° to 0.5° in the immediate vicinity of the discontinuities and still belong entirely within the low structural state.

Acknowledgments

This study was supported in part by the Research Committee of the Graduate School from funds supplied by the Wisconsin Alumni Research Foundation. The authors wish to express their appreciation to R. C. Emmons, H. S. Yoder, Jr., H. H. Hess, R. E. Wilcox, G. A. Desborough, and T. A. Vogel for furnishing the specimens used and to P. H. Ribbe and T. A. Vogel for measuring optical and x-ray data on four specimens.

References

Bown, M. G. and P. Gay (1958) The reciprocal lattice geometry of the plagioclase felspar structures. *Zeit Krist.* **111,** 1–14.

Brown, W. L. (1960*a*) Lattice changes in heat-treated plagioclases—the existence of monalbite at room temperature. *Zeit. Krist.* **113,** 297–329.

——— (1960*b*) The crystallographic and petrologic significance of peristerite unmixing in the acid plagioclases. *Zeit. Krist.* **113,** 330–344.

Crump, R. M. and K. B. Ketner (1953) Feldspar optics, p. 23–40 in *Selected Petrogenic Relationships of Plagioclase. Geol. Soc. Am. Mem.* **52.**

Duparc, L. and M. Reinhard (1924) La determination des plagioclases dans les coupes minces. *Soc. Phys. Hist. Nat. Geneve Mem.* **40.**

Emmons, R. C. (1953) Selected petrogenic relationships of plagioclase. *Geol. Soc. Am. Mem.* **52.**

——— R. M. Crump and K. B. Ketner (1960) High- and low-temperature plagioclase. *Geol. Soc. Am. Bull.* **71,** 1417–1420.

Gay, P. (1953) The structures of the plagioclase felspars: III. An X-ray study of anorthites and bytownites. *Mineral. Mag.* **30,** 169–177.

——— (1962) Sub solidus relations in the plagioclase feldspars, *Norsk Geol. Tidsskr.* **42**(2), 37–56.

——— and M. G. Bown (1956) The structures of the plagioclase felspars: VII. The heat treatment of intermediate plagioclases. *Mineral. Mag.* **31,** 306–313.

Glauser, A. (1961) Zur Orientierung der Indikatrix im Plagioklas-Material von R. C. Emmons. *Schweiz. Mineral. Petrogr. Mitt.* **41,** 443–470.

Goodyear, J. and W. J. Duffin (1954) The identification and determination of plagioclase felspars by the x-ray powder method. *Mineral. Mag.* **30,** 306–326.

Kempster, C. J. E., H. D. Megaw and E. W. Radoslovich (1962) The structure of anorthite, $CaAl_2Si_2O_8$. I. Structure analysis. *Acta Cryst.* **15,** 1005–1017.

Megaw, H. D. (1960) Order and disorder I. Theory of stacking faults and diffraction

maxima. II. Theory of diffraction effects in the intermediate plagioclase felspars. III. The structure of the intermediate plagioclase felspars. *Proc. Royal Soc.* **A259,** 59–78, 159–183, 184–202.

——— (1962) Order and disorder in felspars. *Norsk. Geol. Tidsskr.* **42,** 104–137.

MOOKHERJEE, A. AND K. C. SAHU (1960) Microhardness of the plagioclase series. *Am. Mineral.* **45,** 742–744.

REYNOLDS, D. L. (1952) The difference in optics between volcanic and plutonic plagioclases, and its bearing on the granite problem. *Geol. Mag.* **89,** 233–250.

RIBBE, P. H. (1960) An *x*-ray and optical investigation of the peristerite plagioclases. *Am. Mineral.* **45,** 626–644.

——— (1962) Observations on the nature of unmixing in peristerite plagioclases. *Norsk Geol. Tidsskr.* **42**(2), 138–151.

SMITH, J. R. (1958) The optical properties of heated plagioclases. *Am. Mineral.* **43,** 1179–1194.

——— (1960) Optical properties of low-temperature plagioclase, in *Stillwater Igneous Complex, Montana,* H. H. Hess, *Geol. Soc. Am. Mem.* **80,** 191–219.

——— AND H. S. YODER, JR. (1956) Variations in *x*-ray powder diffraction patterns of plagioclase feldspars. *Am. Mineral.* **41,** 632–647.

SMITH, J. V. (1956) The powder patterns and lattice parameters of plagioclase felspars. I. The soda-rich plagioclases. *Mineral. Mag.* **31,** 47–68.

——— (1958) The effect of composition and structural state on the rhombic section and pericline twins of plagioclase felspars. *Mineral. Mag.* **31,** 914–928.

——— AND P. GAY (1958) The powder patterns and lattice parameters of plagioclase felspars. II. *Mineral. Mag.* **31,** 744–762.

TAYLOR, W. H., J. A. DARBYSHIRE AND H. STRUNZ (1934) An *x*-ray investigation of the felspars. *Zeit. Krist.* **87,** 464–498.

THOMPSON, C. S. AND M. E. WADSWORTH (1957) Determination of the composition of plagioclase feldspars by means of infrared spectroscopy. *Am. Mineral.* **42,** 334–341.

TOMISAKA, T. (1959) Structural and genetical studies on feldspar group (Part 2). *Sci. Report Yamaguchi Univ.* **10,** 21–71.

VAN DER KAADEN, G. (1951), Optical studies on natural plagioclase feldspar with high-temperature and low-temperature optics. Ph. D. thesis, Univ. Utrecht.

VOGEL, T. A. (1964) Optical-crystallographic scatter in plagioclases. *Am. Mineral.* **49,** 614–633.

WILCOX, R. E. (1959) Use of spindle stage for determining refractive indices of crystal fragments. *Am. Mineral.* **44,** 1272–1293.

Manuscript received, August 4, 1964; accepted for publication, April 1, 1965.